Experimental study on the synthesis and characterization of volcanic rocks (pozzolan and perlite)-based geopolymers

Ayoub AZIZ (Ayoubaziz100@gmail.com)
Mohammed V University of Rabat Scientific Institute: Universite Mohammed V de Rabat Institut Scientifique

Abdellah BENZAOUAK
UM5R ENSET: Universite Mohammed V de Rabat Universite Ecole Normale Superieure de l'Enseignement Technique de Rabat

Abdelilah BELLIL
UM5R IS: Universite Mohammed V de Rabat Institut Scientifique

Thamer ALOMAYRI
UAQU: Umm Al Quwain University

Iz-Eddine EL AMRANI EL HASSANI
UM5R IS: Universite Mohammed V de Rabat Institut Scientifique

Mohammed ACHAB
UM5R IS: Universite Mohammed V de Rabat Institut Scientifique

Mohammed FEKHAOUI
UM5R IS: Universite Mohammed V de Rabat Institut Scientifique

Research Article

Keywords: Pozzolan, Perlite, Geopolymer, Physico-chemical proprieties, Building materials

Posted Date: March 19th, 2021

DOI: https://doi.org/10.21203/rs.3.rs-316741/v1

Abstract

The geopolymer preparation based on natural pozzolan is a promising route. Thus, improving the physicochemical properties of these geopolymers by adding other volcanic rocks merits investigation. The present work aims to study the effect of perlite addition, as an acidic volcanic rock, on the physico-chemical and microstructural properties of geopolymers based on pozzolan (basic volcanic rock). The perlite proportion varied between 0 and 50%. A mixture of sodium silicate (Na_2SiO_3) and sodium hydroxide (NaOH) was used as an alkaline activator. The perlite effect on the physico-mechanical properties of the synthesized geopolymers was evaluated by the compressive strength (Rc), *P*-wave velocity (Vp), bulk density (*D*), and porosity (*P*). The microstructural aspects have been explored by X-ray Diffractometry (XRD), Infrared Spectroscopy (FT-IR), Scanning Electron Microscopy (SEM), and Energy-Dispersive X-ray spectroscopy (EDS). The results highlight the possibility of obtaining an eco-efficient geopolymer, with compressive strength of up to 50 MPa at 28 days by partially replacing the pozzolan by 40% of the perlite, due to the formation of more amorphous N-A-S-H type gel. However, the excessive content (over 40%) of perlite had a negative effect on the development of the compressive strength and microstructure of the pozzolan-based geopolymer, which was related to the formation of zeolitic phases in the geopolymer matrix. This study confirms the promise of using pozzolan-perlite-based geopolymers as sustainable building materials, which could significantly promote the development of geo-resources and environmental protection in the construction sector.

1. Introduction

With population growth, the demand for building materials has grown steadily, especially Portland cement, which remains an energy-intensive and polluting industrial operation [1, 2]. Every second in the world, 146,000 kilos of Portland cement are poured, i.e. 4.6 billion tons per year, with an estimated CO_2 emission of one ton per ton of cement produced, i.e. the release of 4.6 billion tons of CO_2 per year (*Planetoscope, real-time global statistics*). These make cement companies one of the main producers of greenhouse gases (8% of the world's CO_2) [3]. In order to deal with the ecological crises linked to the production of Portland cement, the trend towards the search for new ecological building materials has developed considerably over the last few decades, mainly "geopolymers".

Geopolymers are relatively environmentally friendly cementitious materials, synthesized by a chemical reaction between silica and alumina-rich precursors and an activator solution [4, 5]. In the alkaline solution, the precursors are dissolved to produce aluminates and silicates. These, with the reaction development, are alternately bound to form the three types of geopolymer products: poly(sialate) [–SiO_4–AlO_4–], poly(sialate-siloxo) [–SiO_4–AlO_4–SiO_4–], and poly(sialate-disiloxo) [–SiO_4–AlO_4–SiO_4–SiO_4–] [6]. Geopolymers have several properties compared to Portland cement: high compressive and flexural strength, low shrinkage, low permeability; high resistance to fire and aggressive environments and high durability [6, 7]. Because of these properties, geopolymer applications cover many fields: ceramics [8, 9], concrete [10, 11], insulation [12, 13], stabilization and sorption of hazardous waste [14, 15], etc. These

depend on many factors, including the nature and chemico-mineralogical composition of the raw materials. Several alumino-silicate sources have been used in the synthesis of geopolymers such as kaolinic clays [16, 17], red clays [18, 19], pozzolan [20, 21], perlite [22, 23], etc.

Natural pozzolan and natural perlite are volcanic rocks appropriate for the synthesis of geopolymers. Natural pozzolan is a basic (% SiO_2 < 52) vacuolar volcanic product of Strombolian basaltic eruptions (explosive) containing a small amount of amorphous phase. Pozzolan has been used by several authors for the synthesis of geopolymers [1, 24–26]. However, the results are not satisfactory due to its crystalline nature. In other respects, natural perlite is an amorphous rhyolitic rock of basic character (68% ≤ SiO_2 ≤ 78%) produced by brutal cooling of the viscous magmatic liquid. Contrary to pozzolan, perlite has a vitreous texture, but the research works carried out on the synthesis of geopolymers based on this volcanic rock remain few [22, 23, 27, 28].

The objective of this work is to study the addition effect of an acidic volcanic rock (perlite) on the physico-chemical and microstructural properties of geopolymers based on a basic volcanic rock (pozzolan). From a methodological point of view, firstly, the chemico-mineralogical characterization of the two volcanic rocks was carried out using XRF analysis, thin-sections analysis, FT-IR analysis, and XRD analysis. Series of geopolymers were then synthesized by adding increasing levels of perlite to the pozzolan. Finally, the geopolymers obtained were subjected to a series of physico-mechanical (Rc, Vp, *D*, *P*) and microstructural (XRD, FT-IR, SEM, EDS) analyses in order to study the synergy between pozzolan and perlite in the synthesis of geopolymers. Furthermore, this work aims to enhance the value of pozzolan and perlite, two volcanic rocks that are abundant in nature, whose exploitation contributes to the creation of socio-economic spin-offs in volcanic regions.

2. Materials And Methodology

2.1 Materials

Natural pozzolan: The natural pozzolan used in this study originated from the volcanic chain of the Moroccan Middle Atlas, located between the cities of Azrou and Timahdite (33°21'29.8"N 05°09'01"W), in which several pozzolan deposits are found, linked to the different volcanic vents (cones and maars) (Fig. 1D). Natural volcanic pozzolan is characterized by granular appearance, with a rather friable vacuolar structure and a mixed texture of a crystalline and an amorphous fraction, formed by the projection of gas-rich lava fragments into the air during the explosive phases of the volcanic activity that affected different regions of Morocco (Rif, Atlas, and the Meseta) from the Middle Neogene (16 Ma) onwards [29]. The pozzolan was crushed to a particle size of less than 63µm.

Natural perlite: The natural perlite used is sampled from the north-eastern Rif, more precisely from the city of Nador (x: 33°01'46.60 "N; y: 04°56'25.62O; Alt.: 501 m) (Fig. 1C). Perlite is an amorphous volcanic rock, light grey, greenish or black in color, whose petrographic composition is that of a hydrated rhyolitic,

resulting from the obsidian hydration and other volcanic glass. This perlite has a grain size of less than 63µm.

Activator solution: The mixture of sodium hydroxide solution (NaOH) and sodium silicate solution (Na_2SiO_3) was used as an alkaline activator. The sodium hydroxide solution with a molarity of 8M was prepared by mixing 97-98% pure pellets with distilled water. The sodium silicate solution used is composed of 25.7% SiO_2, 10.2% Na_2O, and 64.1% H_2O with a bulk density of 1370 kg/m^3. The prepared batch was kept, subsequently, at room temperature for 24 hours before manipulation.

2.2. Geopolymers preparation

The synthesis method of geopolymer cements in this study has been schematized in Fig. 2. Geopolymer composites based on pozzolan (P) and perlite (Pr) are synthesized by incorporating percentages of perlite in the pozzolan. The two precursors were crushed using a ball mill and sieved to a particle size of less than 63m, then 6 batches of the dry mix were prepared by replacing the pozzolan with increasing perlite contents (0, 10, 20, 30, 40, and 50%). The activator solution (NaOH [8M], Na_2SiO_3/NaOH=1), previously prepared, was added to each batch with a liquid/solid ratio equal to 0.5 and homogenized for 10 min. Following that, the mixtures were poured into cylindrical plastic molds (CPVC; 2 cm diameter and 4 cm height) and vibrated to remove the air bubbles inserted in the mixtures. The filled molds are thermally cured at a temperature of 60 °C for 24 hours. After 24 hours of curing, the samples were removed from the molds and packed in special plastic bags until the test age.

2.3. Characterization methods

2.3.1. XRF analysis

The chemical composition of the raw materials used was determined in mass percentage using an AXIOS spectrometer (CNRST-UATRS).

2.3.2. XRD analysis

The mineralogical analysis of the raw materials and the synthesized geopolymers were examined by X-ray diffraction using a Panalytical XPERT PRO diffractometer (CNRST-UATRS), operating by copper Kα1 radiation reflection (λ = 1.54056 Å).

2.3.3. FTIR analysis

The infrared analysis of raw materials and geopolymers was carried out using a BRUKER VERTEX 70 type spectrometer (CNRST-UATRS). The analyses were performed in transmittance mode in a wavenumber region 400-4000 cm^{-1}.

2.3.4. Bulk density and porosity

The bulk density and porosity of the synthesized geopolymers were determined, according to ASTM C642-13, at 28 days of curing. For each formulation, three geopolymer samples were tested, and the mean velocity was considered as the representative value.

2.3.5. Compressive strength

The compressive strength of the synthesized geopolymers was determined in cylindrical samples (2 cm diameter and 4 cm high) after 7 and 28 days of curing using a hydraulic press (RP25 ATF- ASTM 1231 standard (2010)) with a compression capacity of 25 kN and loading rate of 1.6 kN/sec. For each formulation, three replicate samples were tested, and the average mechanical strength was considered as the representative value.

2.3.6. P-wave velocity

The P-wave velocity measurements on the geopolymers, 28 days of curing, were carried out using a TICO-type instrument (NFP 94-411), consisting of an ultrasonic wave generator (0.1-6500 µs; 1 pulse/s) along with two piezoelectric transducers. For each formulation, three replicate samples were tested.

2.3.7. SEM/EDX analysis

The morphology of the synthesized geopolymers was analyzed using a scanning electron microscope coupled, with an energy dispersive X-ray spectrometer of the JEOL JSMTT 100 type. A gold ultra-thin layer (2.5nm) was deposited on the specimens by a secondary vacuum metalliser of the JEOL JFC-2300 HR type.

3. Results And Discussion

3.3. Raw materials characterization

3.3.1. Natural pozzolan

The pozzolan fragments used in this study show a low bulk density (Fig. 4a), high porosity, and high water absorption of around 1100 kg/m^3, 54%, and 13%, respectively. From a chemico-mineralogical point of view, the chemical analysis of the pozzolan shows the composition of a basic rock (SiO_2 = 37%), moderately aluminous (Al_2O_3 = 15%), strongly ferromagnesium-titanium-bearing (Fe_2O_3 + MgO + TiO_2 = 28%), and more calcareous than alkaline (CaO/ (Na_2O+K_2O) = 6.62) (Fig. 3a). Microscopic analysis of thin-section of pozzolan fragments under a polarizing microscope showed a vacuolar texture (V) (Fig. 4c), appearing in white and a vitreous matrix (M), showing in black, punctuated with microlites of feldspathic plagioclases (PL), diopside (Px), amphibole (Am), and opaque micro grains (hematite). Mineralogical analysis by X-ray diffraction corroborates the observation results of the thin-section and showed the presence of small amounts of amorphous phase as well as the crystalline phase well expressed in peaks of varying intensity (Fig. 5), corresponding to microlites of plagioclase (anorthite), calco-magnesian pyroxene (augite), iron oxides (hematite), and olivine (forsterite). FT-IR analysis also

confirmed the mineral phases revealed by the XRD (anorthite, augite), by the manifestation of the absorption bands around 537 cm^{-1} and 460 cm^{-1} (Fig. 6); this reflects the presence of Si-O-Al and Si-O-Si bending vibrations, and the absorption band around 1042 cm^{-1}, which corresponds to the asymmetrical and symmetrical stretching vibrations of the Si-O-Si and Si-O-Al links.

3.3.2 Natural perlite

The centimetric perlite fragments had a high bulk density of around 2300 kg/m^3 (Fig. 4b), a low porosity varying about 1.5%, and a low water absorption rate of 0.66%. The chemical composition of the perlite, determined by XRF, showed that it is an acidic siliceous rock (SiO_2= 73.46%), moderately aluminous (Al_2O_3=13.15%), and with a sodi-potassic character ($Na_2O + K_2O$ = 3.33%) (Fig. 3b). The observation of thin-segments of the perlite under the polarizing microscope had shown a hyaline texture (amorphous) (Fig. 4d), punctuated by a few tiny grains and microlites of plagioclase, which corroborates the XRD results (Fig. 5), revealing the amorphous texture of the perlite, attested by the presence of an amorphous phase halo with a few peaks corresponding to the microcrystals of anorthite and quartz. The pozzolan infrared spectrum (Fig. 6), conducted by FTIR analysis, showed the presence of bands around 1000, 94 cm^{-1} and 780 cm^{-1}, corresponding respectively to the Si-O-Si and Si-O-Al bonds' stretching vibrations, and a band at 460 cm^{-1} attributed to bending vibration of the Si-O-Si bond. The bands displayed at 3456 cm^{-1} and 1639 cm^{-1} are assigned respectively to the bending vibration of the H-O-H bond and the stretching vibration of the -OH bond.

3.4. Characterization of geopolymer products

3.4.1. Macroscopic appearance

Cylindrical samples of the synthesized geopolymers are presented in Fig. 7. Macroscopic observation of pozzolan-perlite-based geopolymers shows satisfactory solidification without surface cracking or efflorescence, except for the G50 geopolymer which shows a very cracked matrix. Their colors vary from light yellow to light grey as the percentage of perlite increases. As the addition of 50% perlite to the pozzolan resulted in cracked specimens, the perlite addition has been limited to 50%.

3.4.2. Compressive strength analysis

The results presented in Fig. 8 show that the compressive strengths of all synthesized geopolymers increased with the curing age (from 7 to 28 days of curing), with an average rate of increase of 27%. In detail, the 10% perlite addition to the pozzolan resulted in a relatively significant improvement in Rc from 12.56 MPa to 17 MPa at 7 days and from 14 MPa to 18.6 MPa at 28 days of curing. The progressive increase of the perlite content from 10% to 40% has considerably increased the Rc of the samples, which reached 50 MPa for 40% perlite after 28 days of curing. From 40% to 50% perlite, the Rc evolved negatively by a decrease of 18% (from 50 MPa to 41 MPa for 28 days of curing). It means that the G40 specimen is the mechanically optimal geopolymer. This indicates that the addition of natural perlite, at the 40% level, has contributed to the compressive strength development of the synthesized geopolymers,

presumably related to the additional reaction resource obtained from the perlite. The increase in the compressive strength with the perlite incorporation was due to the relatively higher SiO_2/Al_2O_3 molar ratio and the amorphous nature of perlite compared to pozzolan [1, 30, 31], which increases the content of reactive silica and alumina in the reaction medium and, consequently, the formation of more geopolymerization products, which could be mainly sodium aluminosilicate hydrate gel (N-A-S-H) due to the low calcium content [30, 32]. These results are in accordance with those found by Duan et al, [33], which show the increase in compressive strength of fly ash-based geopolymers with increasing silica fume content. It should be noted that the geopolymerization reaction of perlite could produce co-products of zeolitic nature. This has been observed in the works of Vance et al., [23], Taxiarcho et al., [28], Kozhukhova et al., [27], who detected the formation of the zeolitic phases, particularly phillipsite, in geopolymers based on natural perlite. Hence, the decrease in compressive strength observed in the present study beyond 40% perlite could be related to the appearance of zeolitic phases in the geopolymer matrix, leading to the formation of a heterogeneous structure and, consequently, the decrease in the mechanical properties [34–37].

3.4.3 Bulk density and porosity analysis

Table 1 shows the bulk density and porosity results according to the perlite content added to the pozzolan. Based on physical laws, bulk density varies inversely with porosity, which is explicitly shown in the case of this study. The bulk density and porosity variation of the geopolymers synthesized in this study is consistent with the trend observed from mechanical properties, which is justified by the high positive correlation between density and Rc (R^2=0.99) (Fig. 9). The partial replacement of pozzolan by perlite, from 10 to 40%, resulted in an increase in bulk density from 1813 g/cm^3 to 2055 g/cm^3, correlated to a decrease in porosity from 14% to 9.71%. These results can be attributed to the formation of geopolymerisation products such as N-A-S-H gel as a function of the perlite addition (≤40%), hence the densification of the geopolymer matrix [38]. The increase in the perlite content, from 40% to 50%, decreases the density, from 2055 g/cm^3 to 1987 g/cm^3, and increases the porosity, from 9.71% to 10.77%, which is linked, according to Nuaklong et al. [39], to the weak zones formation, thus affecting the mechanical properties of the synthesized geopolymers.

3.4.4 P-wave velocity analysis

The *P*-wave propagation velocities (Vp) measured at 28 days of curing are shown in Fig.10. The results show that the Vp velocity increases, from 3133 m/s to 4055 m/s, with the increase in perlite content, from 10% to 40%, while the addition of more than 40% perlite decreases the *P*-wave velocity, from 4055 m/s to 3615 m/s, a velocity lower than that of the G30 geopolymer. The increase in Vp shows that the internal structure becomes denser and more homogeneous by increasing the pearlite content to 40%, which explains the good *P*-wave propagation [29, 40]. The decrease in Vp observed by the addition of more than 40% of perlite is due, according to El Azhari and El Hassani [41] and Garnier et al., [42], to the existence of discontinuities in the geopolymers. These results are in agreement with macroscopic observations (Fig. 7), measurements of bulk density (Table 1), and compressive strength (Fig. 8), showing that the perlite

addition up to a content of 40% leads to the formation of a dense and homogeneous matrix, which increases the compressive strength, and consequently, the increase of Vp in the synthesized geopolymers. Above 40% perlite, cracks in the G50 geopolymer matrix were well highlighted in Fig. 7, which is at the origin of the *P*-wave velocity decrease. Similarly, the linear regression results showed a positive correlation between Vp and Rc of the synthesized geopolymers, represented by the determination coefficient R^2, which was of the order of 0.95 (Fig. 9).

3.4.5. XRD analysis

The X-ray diffractograms of the synthesized geopolymers as a function of perlite content are shown in Fig. 11. A large halo has been detected in all perlite-pozzolan-based geopolymer composites between 20°-40° (2θ) indicating the formation of a glassy phase in the system [1, 43, 44]**.** In detail, the amorphous phase halo increase is proportional to the perlite percentage added, which shows the contribution of perlite to the more formation of the binder phase (N-A-S-H) in composites elaborated by its siliceous and vitreous nature, which consequently leads to the increase of the mechanical properties of the synthesized geopolymers (Fig. 11a) [45, 46]. This tendency was well demonstrated in the study conducted by Zhuen et al., [47] by integrating up to 15% of rice husk ash into the fly ash-based geopolymer. Besides, the partial replacement of pozzolan by perlite leads to the appearance and disappearance of crystalline phases. In the case of optimal geopolymer G40 (Fig. 11b), the decrease and disappearance of some peaks corresponding to anorthite, hematite, and augite, were detected after the geopolymerization reaction. According to Aziz et al., and Robayo-Salazar et al., [1, 29, 46]**,** this behavior was related to the partial dissolution of these crystalline phases and their involvement in the formation of the N-A-S-H geopolymer phase. The appearance of the phillipsite-type zeolite phase (2q = 13.88°, 16.54°, 30.38°, 32.45°, 37.55°) has been observed by increasing the percentage of perlite up to 50%, which is also observed in the work of Aziz et al., and Moon et al., [29, 48]. Therefore, this zeolitic phase neo-formation is at the origin of the decrease in compressive strength exceeding 40% of the perlite (Fig. 8), favoring the formation of more zeolite phase in the geopolymer matrix (N-A-S-H) forming a heterogeneous microstructure, and consequently, the cracks appearance, which is observed in the macroscopic aspect of the G50 sample, hence the decrease in mechanical properties [28].

3.4.6 FT-IR analysis

The infrared spectra of the raw materials (pozzolan and perlite) and the mechanically optimal geopolymer G40 are presented in Fig. 12. From Fig. 12, it appears that the large absorption bands located at 3456 cm^{-1} and the less pronounced at 1639 cm^{-1} on the spectra of G40 and pozzolan, are assigned to the vibration modes of O-H bonds belonging to water molecules [49]. The absorption bands situated between 1384 and 1440 cm^{-1}, are linked to the C-O stretching of the CO_3^{2-} group [50]. These bonds are formed from a reaction between an unfixed Na^+ into a geopolymer matrix with CO_2 of the atmosphere [51, 52]. The absorption bands appearing around 1042 cm^{-1} in all spectra are linked to vibration modes of Si-O-Al bonds [53]. This absorption band is higher than those found in literature based on other aluminosilicates such as metakaolin, fly ash, etc. which is near to 1000 cm^{-1} [54, 55]. Thus, the

incorporation of 40% by weight of the reactive perlite in the pozzolan allowed the incorporation of high content of Si- species that made this band shifted, as indicated in Fig. 12, towards the lower wavenumbers compared to that of pozzolan. A comparable tendency was observed by the findings of Kaze et al., [56] and Kamseu et al., [50] where they used reactive silica from rice husk ash to improve the formation of iron silicate compounds from raw iron-rich laterites cured at 80 °C. Also, this shift has been well demonstrated in the geopolymers synthesized by Tawatchai et al., [57], with the increase of the glass waste powder percentage in their fly ash-based geopolymer. In the case of the G40 sample, this band is more pronounced and indicates the formation of the N-A-S-H geopolymer phase required to ensure better connectivity between different particles in the whole system. Moreover, it belongs to the geopolymer network as reported by other researchers justifying that the reaction has taken place [54], which corroborates the compressive strength results found (Fig. 8) that show the increase in mechanical strength with the perlite addition up to 40%.These results correlate with those obtained by XRD (Fig. 11).

3.4.7. SEM/EDS analysis

Fig. 13 represents the SEM micrographs and the corresponding EDS (Energy-Dispersive X-ray Spectroscopy) spectra of geopolymers (G40 and G50) containing high perlite contents. As shown in Fig. 13, the geopolymer with 40% perlite (G40) shows a homogeneous and dense microstructure with few pores and cracks, constituted mainly by the N-A-S-H type geopolymer gel. This was also confirmed by EDS analysis which showed the presence of silica, aluminum, and sodium as major elements with a molar ratio Na/Si=0.49, which was near to the optimum ratio (0.5) for the N-A-S H gel formation [32]; significantly, this contributes to the increase of the mechanical properties of geopolymers [30, 32]. As for the 50% perlite composite geopolymer, its microstructure seems more heterogeneous, porous, and fissured than that of the G40 geopolymer, composed of the N-A-S-H type geopolymer phase, with a molar ratio Na/Si=0.44, and the phillipsite-type zeolitic phase with a prismatic morphology. These results corroborate those found by the XRD (Fig. 11) that show the coexistence of the N-A-S-H phase and the zeolitic phase in synthesized geopolymer cements with a high perlite content (≥40 %) contributing to the formation of a heterogeneous matrix (Fig. 7), and consequently, to the decrease of the mechanical properties of the synthesized geopolymers (Fig. 8) [28].

4. Conclusion

Experimental works on the synthesis of geopolymers based on two volcanic rocks (pozzolan and perlite) from two different volcanism (acid and basic) were carried out in this study. Preliminary synthesis tests of pozzolan-based geopolymers alone resulted in low-structured products with low physical-mechanical characteristics at 28 days of curing (Rc= 14 MPa; Vp= m/s; D= 1778 g/cm^3; P= 14.81%). The partial replacement of pozzolan by up to 40% perlite content significantly improved the properties of the synthesized geopolymers, while the addition of more than 40% perlite decreased the physical-mechanical characteristics. The optimum substitute content of pozzolan by perlite in this research was 40%, in which the compressive strength of the G40 geopolymer reached 50 MPa, the P-wave velocity increased to 4055 m/s, the bulk density became 2052 g/cm^3, and the porosity decreased to 9.71%.

The perlite addition up to 40% content to the pozzolan brought more aluminum and especially reactive silicon into the geopolymerization reaction process, promoting the additional formation of amorphous N-A-S-H type gel. This could be one of the main reasons for the increased mechanical properties of the synthesized geopolymers. With the increase in the perlite percentage (≥ 40%), an appearance of phillipsite-type zeolitic phases has been detected. The coexistence of the zeolitic phase with the geopolymer phase (N-A-S-H) contributes to obtaining a heterogeneous structure. Consequently, the addition of more than 40% of the perlite to the pozzolan increases the amount of phillipsite in the geopolymer matrix which leads to a decrease in mechanical properties.

Declarations

Acknowledgements

This work takes part of the V2GV project framework (Evaluating of Volcanic Geo-Materials and Geo-Sites in Morocco), supported by the Hassan II Academy of Sciences and Techniques (AH2ST). We would like to give it a warm thank you. We sincerely grateful Mrs. Najat MAHIR, Abdelkader AZIZ, and Mrs. Khadija FELAOUS for their support and encouragement. We sincerely grateful Mr. Zakariae Azennoud for his proofreading of this manuscript.

Data Availability: My research didn't generate any data or I reused existing data.

Compliance with Ethical Standards: This article does not contain any studies involving animals or human participants performed by any of the authors.

Conflict of Interest: The authors declare that they have no conflicts of interest.

Consent to Participate: Not Applicable.

Consent for Publication: Not Applicable.

Funding statement: Not Applicable.

References

1. Aziz A, Stocker O, Hassani I-EEAE, et al (2021) Effect of blast-furnace slag on physicochemical properties of pozzolan-based geopolymers. Materials Chemistry and Physics 258:123880. https://doi.org/10.1016/j.matchemphys.2020.123880
2. Bondar D, Lynsdale CJ, Milestone N, et al (2009) Engineering properties of geopolymer concrete based on alkali activated natural pozzolan. In: Proceedings of the Third International Conference on Concrete and Development
3. Akbarnezhad A, Huan M, Mesgari S, Castel A (2015) Recycling of geopolymer concrete. Construction and Building Materials 101:152–158

4. Amran M, Debbarma S, Ozbakkaloglu T (2021) Fly ash-based eco-friendly geopolymer concrete: A critical review of the long-term durability properties. Construction and Building Materials 270:121857
5. Wang Y-S, Alrefaei Y, Dai J-G (2019) Silico-aluminophosphate and Alkali-aluminosilicate Geopolymers: A comparative review. Frontiers in Materials 6:106
6. Davidovits J (1991) Geopolymers: inorganic polymeric new materials. Journal of Thermal Analysis and calorimetry 37:1633–1656
7. Kouamo HT, Elimbi A, Mbey JA, et al (2012) The effect of adding alumina-oxide to metakaolin and volcanic ash on geopolymer products: A comparative study. Construction and Building Materials 35:960–969
8. Lemougna PN, Wang K, Tang Q, Cui X (2017) Synthesis and characterization of low temperature (< 800° C) ceramics from red mud geopolymer precursor. Construction and Building Materials 131:564–573
9. Liew Y-M, Heah C-Y, Li L, et al (2017) Formation of one-part-mixing geopolymers and geopolymer ceramics from geopolymer powder. Construction and Building Materials 156:9–18
10. Nuaklong P, Sata V, Chindaprasirt P (2018) Properties of metakaolin-high calcium fly ash geopolymer concrete containing recycled aggregate from crushed concrete specimens. Construction and Building Materials 161:365–373
11. Zhang HY, Kodur V, Wu B, et al (2018) Effect of temperature on bond characteristics of geopolymer concrete. Construction and Building Materials 163:277–285
12. Colangelo F, Roviello G, Ricciotti L, et al (2018) Mechanical and thermal properties of lightweight geopolymer composites. Cement and Concrete Composites 86:266–272
13. Feng J, Zhang R, Gong L, et al (2015) Development of porous fly ash-based geopolymer with low thermal conductivity. Materials & Design (1980-2015) 65:529–533
14. El-Naggar MR, Amin M (2018) Impact of alkali cations on properties of metakaolin and metakaolin/slag geopolymers: Microstructures in relation to sorption of 134Cs radionuclide. Journal of hazardous materials 344:913–924
15. Van Jaarsveld JGS, Van Deventer JSJ, Lorenzen L (1997) The potential use of geopolymeric materials to immobilise toxic metals: Part I. Theory and applications. Minerals engineering 10:659–669
16. Elimbi A, Tchakoute HK, Njopwouo D (2011) Effects of calcination temperature of kaolinite clays on the properties of geopolymer cements. Construction and Building Materials 25:2805–2812
17. Selmani S, Sdiri A, Bouaziz S, et al (2017) Effects of metakaolin addition on geopolymer prepared from natural kaolinitic clay. Applied Clay Science 146:457–467
18. El Hafid K, Hajjaji M, El Hafid H (2017) Influence of NaOH concentration on microstructure and properties of cured alkali-activated calcined clay. Journal of Building Engineering 11:158–165
19. El Hafid K, Hajjaji M (2016) Alkali-etched heated clay: Microstructure and physical/mechanical properties. Journal of Asian Ceramic Societies 4:234–242

20. ALAHVERDI A, Mehrpour K, NAJAFIKANI E (2008) Taftan pozzolan-based geopolymer cement
21. Ibrahim M, Johari MAM, Maslehuddin M, et al (2019) Influence of composition and concentration of alkaline activator on the properties of natural-pozzolan based green concrete. Construction and Building Materials 201:186–195
22. Erdogan ST (2015) Properties of ground perlite geopolymer mortars. Journal of Materials in Civil Engineering 27:04014210
23. Vance ER, Perera DS, Imperia P, et al (2009) Perlite waste as a precursor for geopolymer formation.
24. Aziz A, El Hassani I-EEA, El Khadiri A, et al (2019) Effect of slaked lime on the geopolymers synthesis of natural pozzolan from Moroccan Middle Atlas. Journal of the Australian Ceramic Society 1–12
25. Robayo-Salazar RA, de Gutiérrez M, Puertas F (2017) Study of synergy between a natural volcanic pozzolan and a granulated blast furnace slag in the production of geopolymeric pastes and mortars. Construction and Building Materials 157:151–160
26. Vafaei M, Allahverdi A (2016) Influence of calcium aluminate cement on geopolymerization of natural pozzolan. Construction and Building Materials 114:290–296
27. Kozhukhova NI, Chizhov RV, Zhernovsky IV, Strokova VV (2016) Structure formation of geopolymer perlite binder vs. type of alkali activating agent. ARPN Journal of Engineering and Applied Sciences 11:12275
28. Taxiarchou M, Panias D, Panagiotopoulou C, et al (2013) Study on the suitability of volcanic amorphous aluminosilicate rocks (perlite) for the synthesis of Geopolymer-based concrete. In: Geopolymer Binder Systems. ASTM International
29. Aziz A, El Amrani El Hassani I-E, El Khadiri A, et al (2020) Effect of slaked lime on the geopolymers synthesis of natural pozzolan from Moroccan Middle Atlas. J Aust Ceram Soc 56:67–78. https://doi.org/10.1007/s41779-019-00361-3
30. Khalid HR, Lee NK, Choudhry I, et al (2019) Evolution of zeolite crystals in geopolymer-supported zeolites: Effects of composition of starting materials. Materials Letters 239:33–36
31. Lau CK, Rowles MR, Parnham GN, et al (2019) Investigation of geopolymers containing fly ash and ground-granulated blast-furnace slag blended by amorphous ratios. Construction and Building Materials 222:731–737
32. Cheah CB, Tan LE, Ramli M (2019) The engineering properties and microstructure of sodium carbonate activated fly ash/slag blended mortars with silica fume. Composites Part B: Engineering 160:558–572
33. Duan P, Yan C, Zhou W (2017) Compressive strength and microstructure of fly ash based geopolymer blended with silica fume under thermal cycle. Cement and Concrete Composites 78:108–119
34. Chindaprasirt P, Paisitsrisawat P, Rattanasak U (2014) Strength and resistance to sulfate and sulfuric acid of ground fluidized bed combustion fly ash–silica fume alkali-activated composite. Advanced Powder Technology 25:1087–1093

35. De Rossi A, Simão L, Ribeiro MJ, et al (2019) In-situ synthesis of zeolites by geopolymerization of biomass fly ash and metakaolin. Materials Letters 236:644–648
36. Rattanasak U, Chindaprasirt P, Suwanvitaya P (2010) Development of high volume rice husk ash alumino silicate composites. International Journal of Minerals, Metallurgy, and Materials 17:654–659
37. Takeda H, Hashimoto S, Yokoyama H, et al (2013) Characterization of zeolite in zeolite-geopolymer hybrid bulk materials derived from kaolinitic clays. Materials 6:1767–1778
38. Kaze CR, Lemougna PN, Alomayri T, et al (2020) Characterization and performance evaluation of laterite based geopolymer binder cured at different temperatures. Construction and Building Materials 121443
39. Nuaklong P, Jongvivatsakul P, Pothisiri T, et al (2020) Influence of rice husk ash on mechanical properties and fire resistance of recycled aggregate high-calcium fly ash geopolymer concrete. Journal of Cleaner Production 252:119797
40. El Hassani IEA, El Azhari H (2009) Evaluation des propriétés physico-mécaniques des pierres de construction du Maroc à partir des vitesses des ondes P et de la résistance au choc. Bulletin de l'Institut Scientifique, Rabat 31:41–54
41. El Azhari H, El Hassani I-EEA (2013) Effect of the number and orientation of fractures on the P-wave velocity diminution: application on the building stones of the Rabat Area (Morocco). Geomaterials 3:71
42. Garnier V, Chaix JF, Rossat M, et al (2009) Caractérisation Non Destructive des bétons par propagation d'ondes ultrasonores. Mechanics & Industry 10:299–303
43. Chindaprasirt P, Rattanasak U (2010) Utilization of blended fluidized bed combustion (FBC) ash and pulverized coal combustion (PCC) fly ash in geopolymer. Waste Management 30:667–672
44. Phoo-ngernkham T, Chindaprasirt P, Sata V, et al (2014) The effect of adding nano-SiO2 and nano-Al2O3 on properties of high calcium fly ash geopolymer cured at ambient temperature. Materials & Design 55:58–65
45. Mehta A, Siddique R (2018) Sustainable geopolymer concrete using ground granulated blast furnace slag and rice husk ash: Strength and permeability properties. Journal of cleaner production 205:49–57
46. Robayo-Salazar RA, de Gutiérrez M, Puertas F (2017) Study of synergy between a natural volcanic pozzolan and a granulated blast furnace slag in the production of geopolymeric pastes and mortars. Construction and Building Materials 157:151–160
47. Zhu H, Liang G, Xu J, et al (2019) Influence of rice husk ash on the waterproof properties of ultrafine fly ash based geopolymer. Construction and Building Materials 208:394–401
48. Moon J, Bae S, Celik K, et al (2014) Characterization of natural pozzolan-based geopolymeric binders. Cement and Concrete Composites 53:97–104
49. Assaedi H, Alomayri T, Kaze CR, et al (2020) Characterization and properties of geopolymer nanocomposites with different contents of nano-CaCO3. Construction and Building Materials

252:119137

50. Kamseu E, Kaze CR, Fekoua JNN, et al (2020) Ferrisilicates formation during the geopolymerization of natural Fe-rich aluminosilicate precursors. Materials Chemistry and Physics 240:122062
51. Mustakim SM, Das SK, Mishra J, et al (2020) Improvement in fresh, mechanical and microstructural properties of fly ash-blast furnace slag based geopolymer concrete by addition of nano and micro silica. Silicon 1–14
52. Nemaleu JGD, Djaoyang VB, Bilkissou A, et al (2020) Investigation of Groundnut Shell Powder on Development of Lightweight Metakaolin Based Geopolymer Composite: Mechanical and Microstructural Properties. Silicon 1–13
53. Tchakouté HK, Melele SJ, Djamen AT, et al (2020) Microstructural and mechanical properties of poly (sialate-siloxo) networks obtained using metakaolins from kaolin and halloysite as aluminosilicate sources: A comparative study. Applied Clay Science 186:105448
54. Nana A, Kaze RC, Alomayri TS, et al Innovative porous ceramic matrices from inorganic polymer composites (IPCs): Microstructure and mechanical properties. Construction and Building Materials 273:122032
55. Youmoue M, Fongang RTT, Gharzouni A, et al (2020) Effect of silica and lignocellulosic additives on the formation and the distribution of meso and macropores in foam metakaolin-based geopolymer filters for dyes and wastewater filtration. SN Applied Sciences 2:1–20
56. Kaze RC, à Moungam LMB, Cannio M, et al (2018) Microstructure and engineering properties of Fe2O3 (FeO)-Al2O3-SiO2 based geopolymer composites. Journal of Cleaner Production 199:849–859
57. Tho-In T, Sata V, Boonserm K, Chindaprasirt P (2018) Compressive strength and microstructure analysis of geopolymer paste using waste glass powder and fly ash. Journal of cleaner production 172:2892–2898

Figures

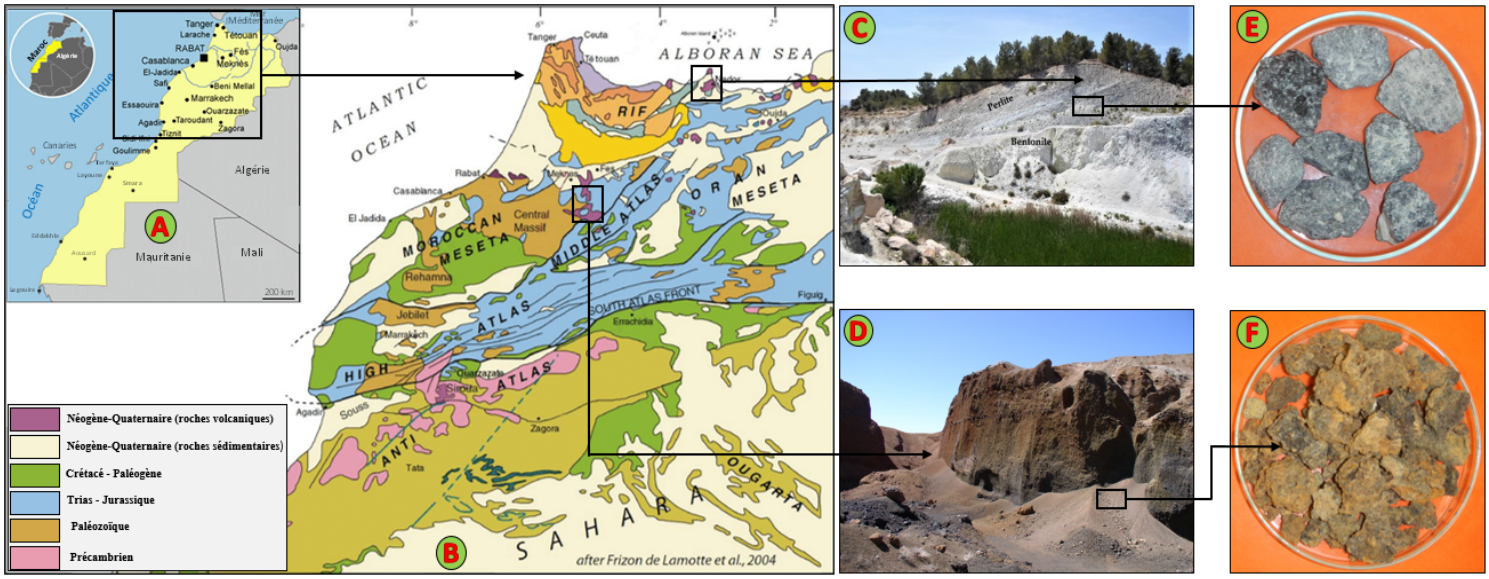

Figure 1

A) Morocco's situation in Africa; B) Zones of origin of pozzolan and perlite on the geological map of northern Morocco; C) View of Nador's perlite quarry; D) View of JbelHebri's pozzolan quarry; E) Macroscopic aspect of the perlite rock; F) Macroscopic appearance of the pozzolan rock

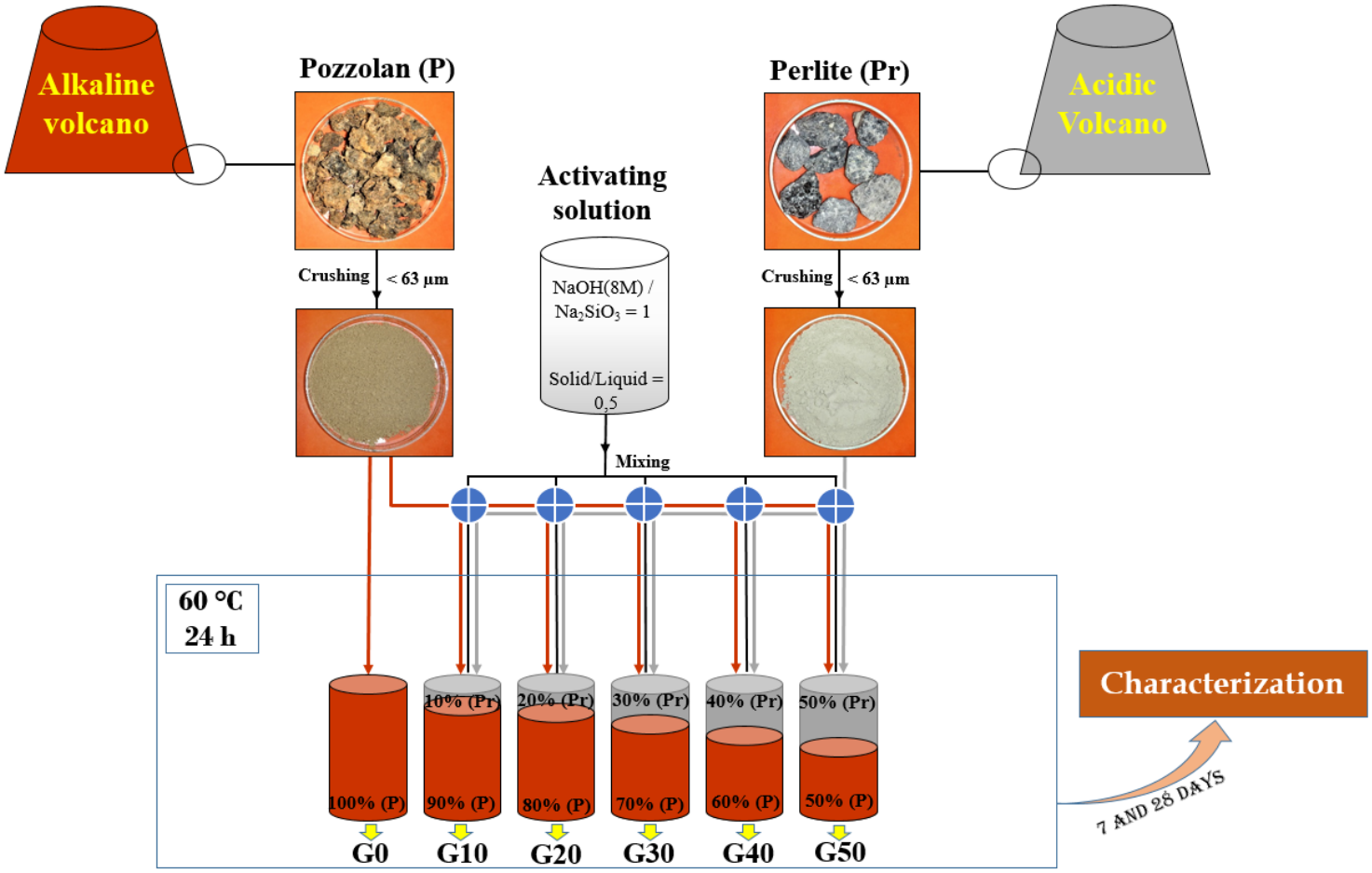

Figure 2

Methodological scheme of the geopolymer synthesis in this study

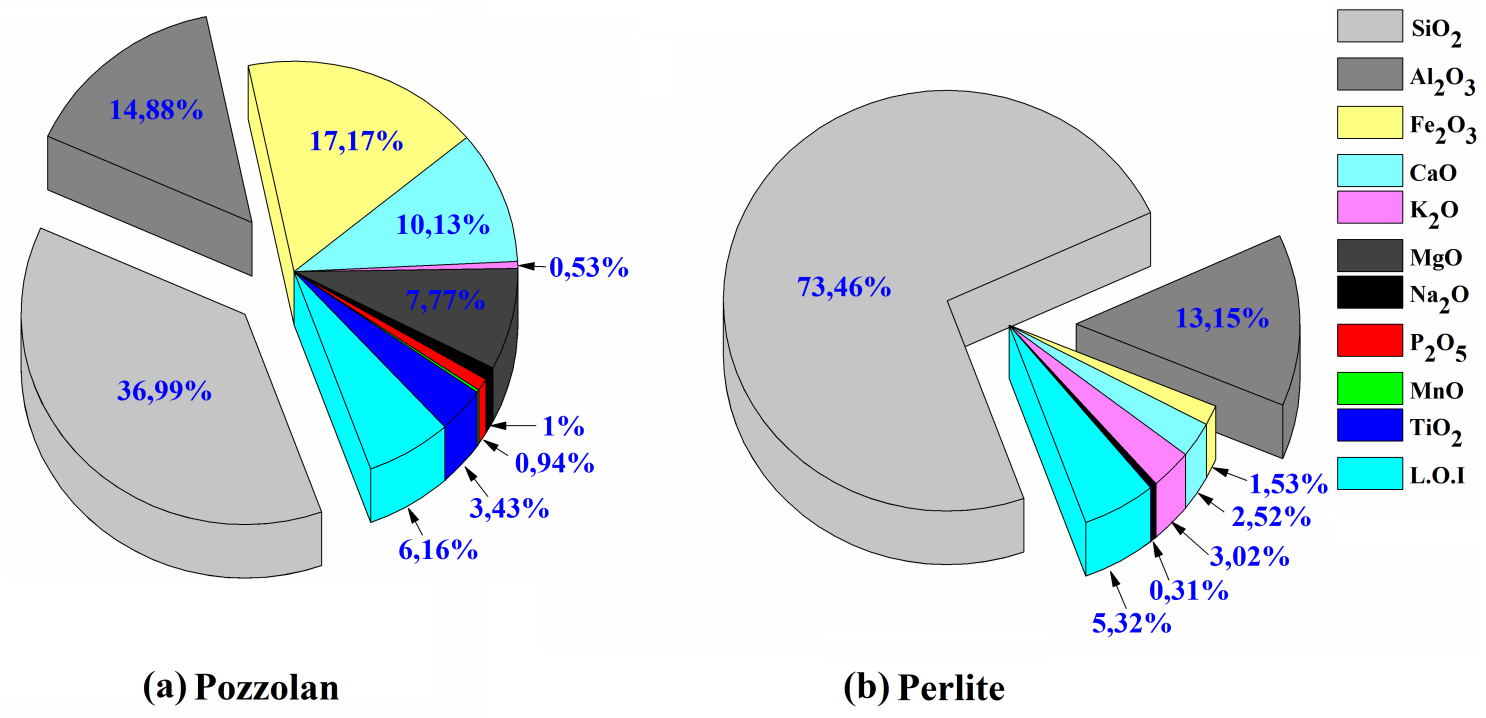

Figure 3

Chemical composition of pozzolan and perlite

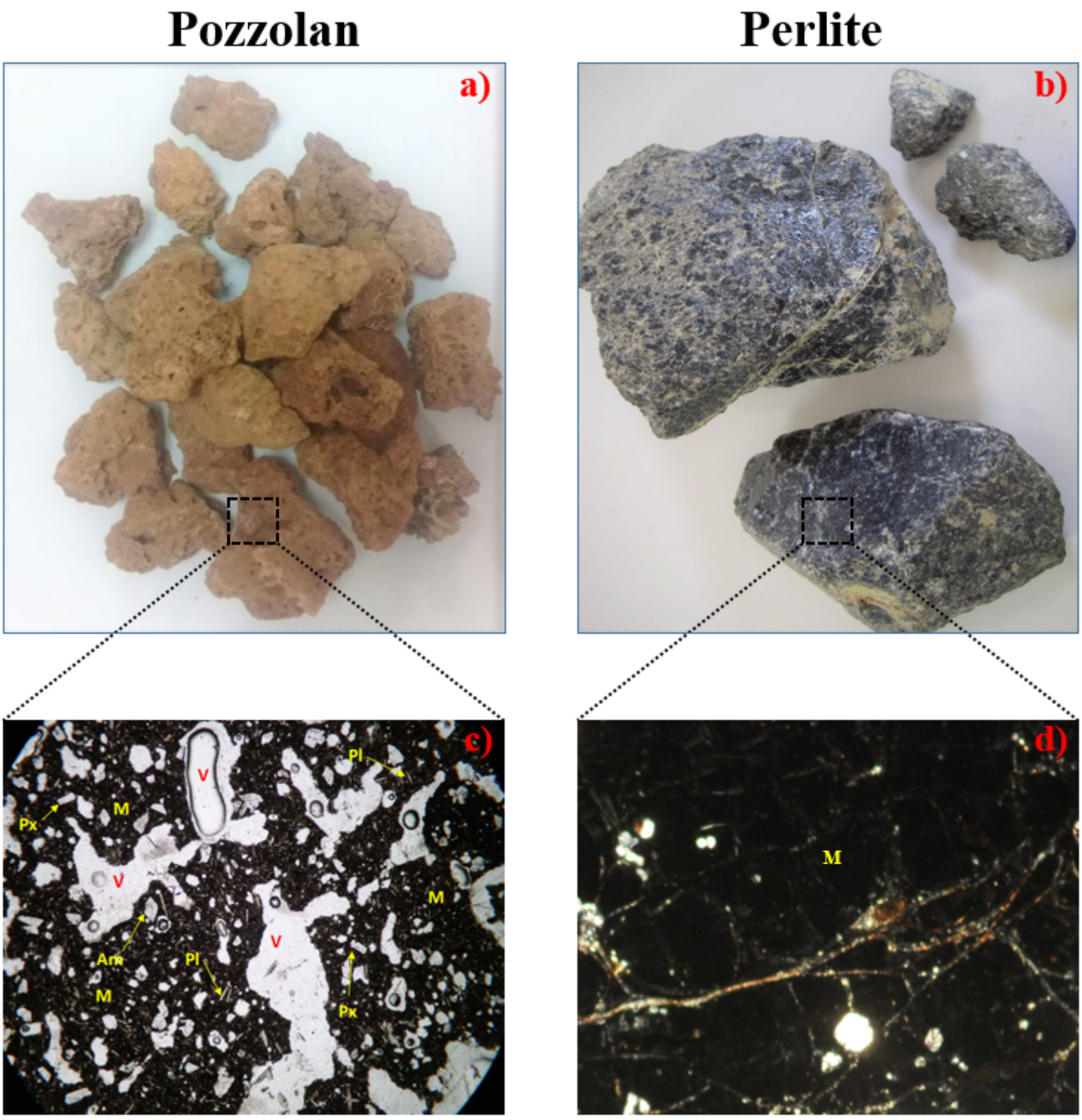

Figure 4

a) Pozzolan fragments; b) Perlite fragments; c) Thin-section of pozzolan; d) Thin-section of perlite

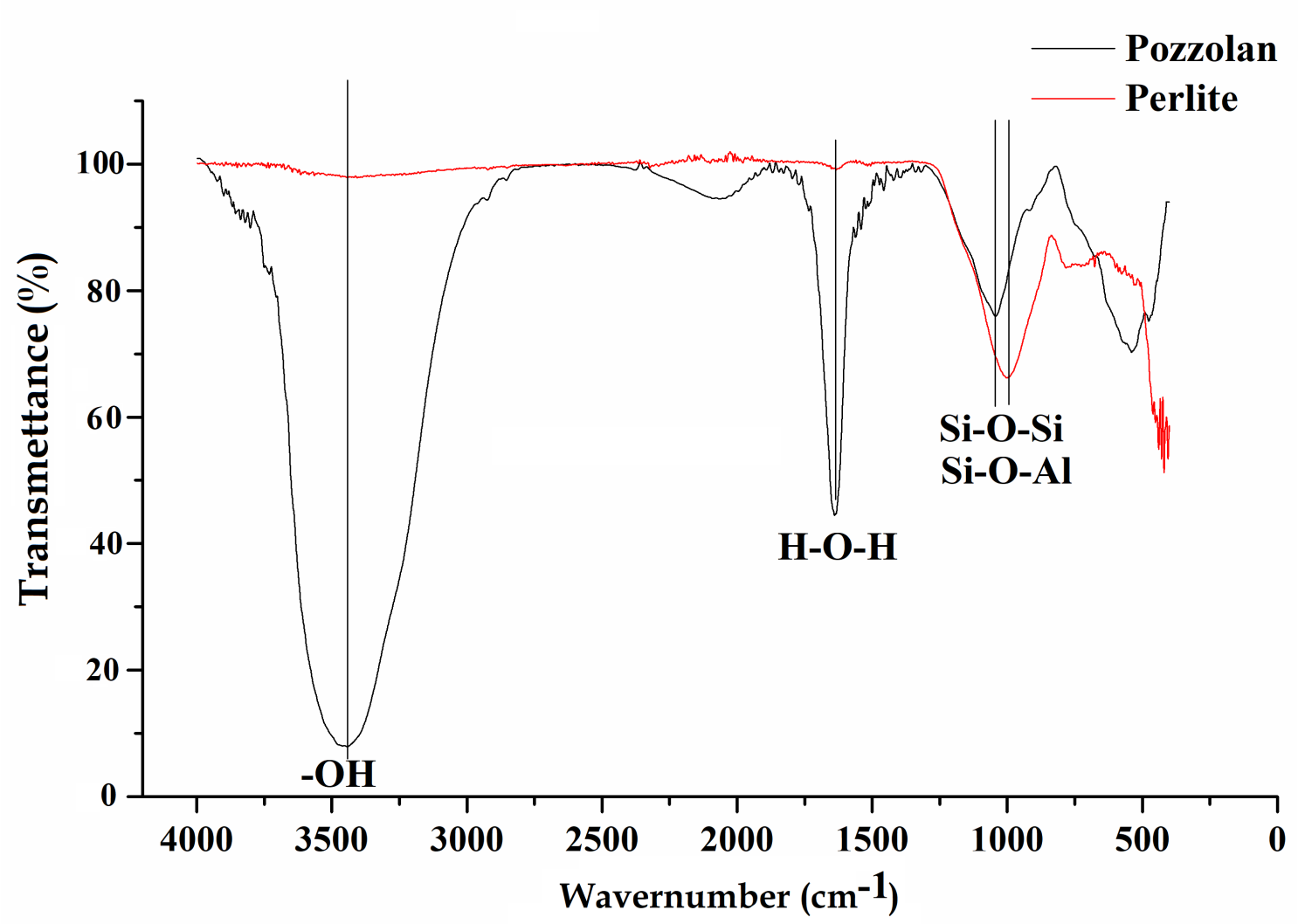

Figure 6

FT-IR spectrum of pozzolan and perlite

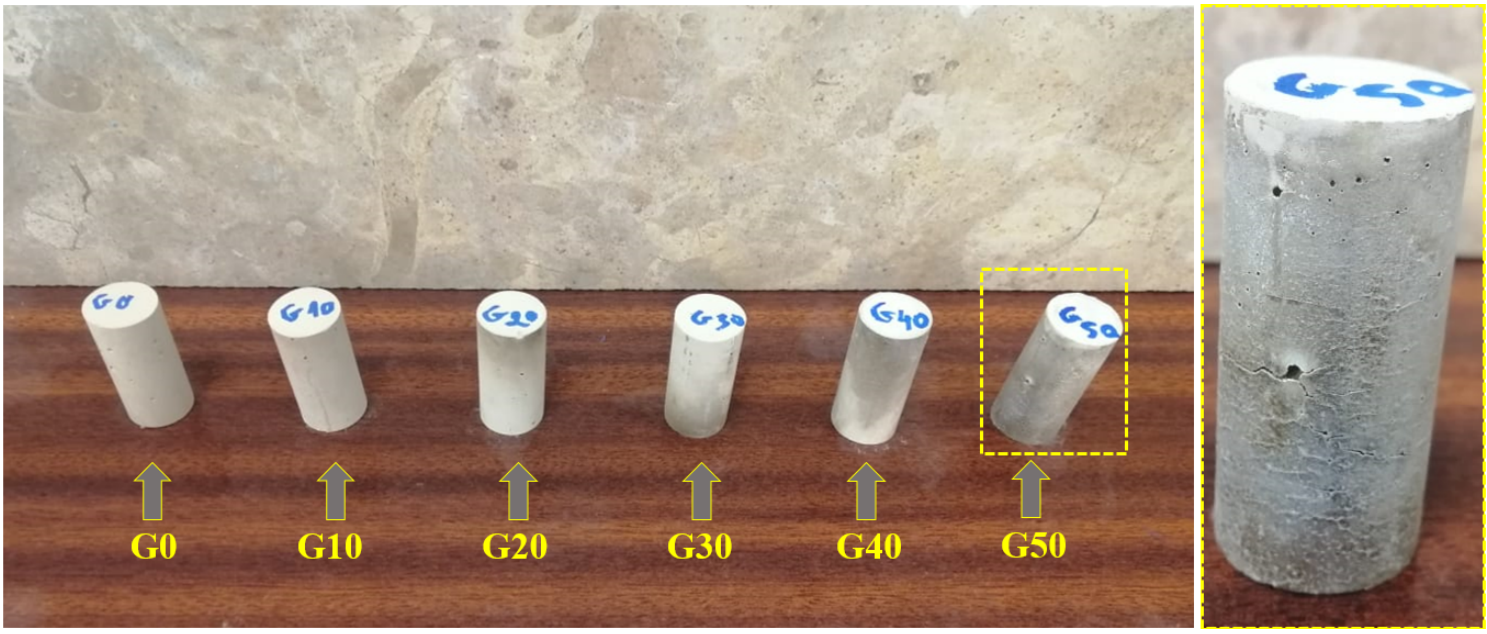

Figure 7

Macroscopic appearance of synthesized geopolymers

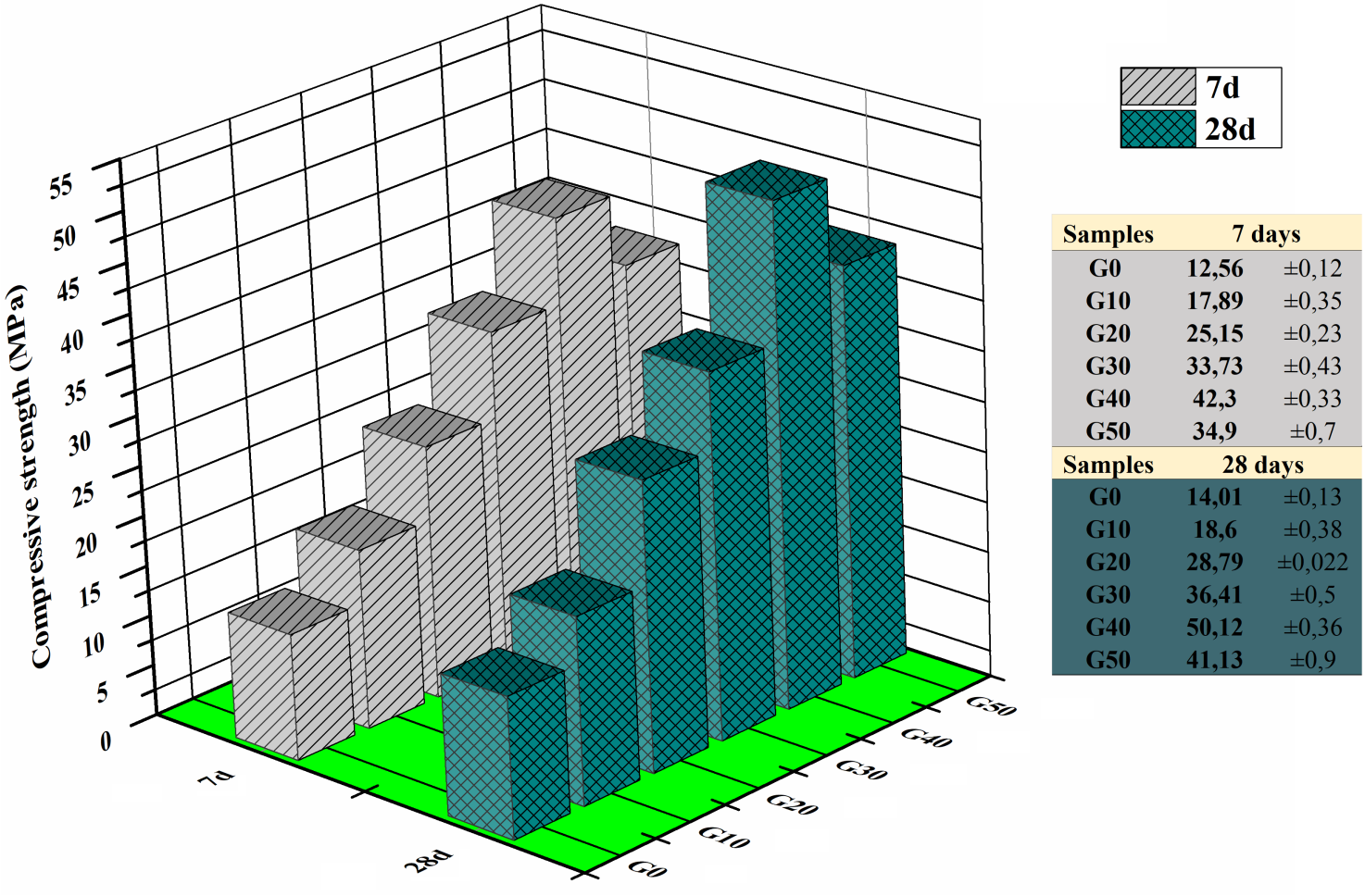

Samples	7 days	
G0	12,56	±0,12
G10	17,89	±0,35
G20	25,15	±0,23
G30	33,73	±0,43
G40	42,3	±0,33
G50	34,9	±0,7
Samples	**28 days**	
G0	14,01	±0,13
G10	18,6	±0,38
G20	28,79	±0,022
G30	36,41	±0,5
G40	50,12	±0,36
G50	41,13	±0,9

Figure 8

Effect of perlite content on the compressive strength of pozzolan-based geopolymers at 7d and 28d

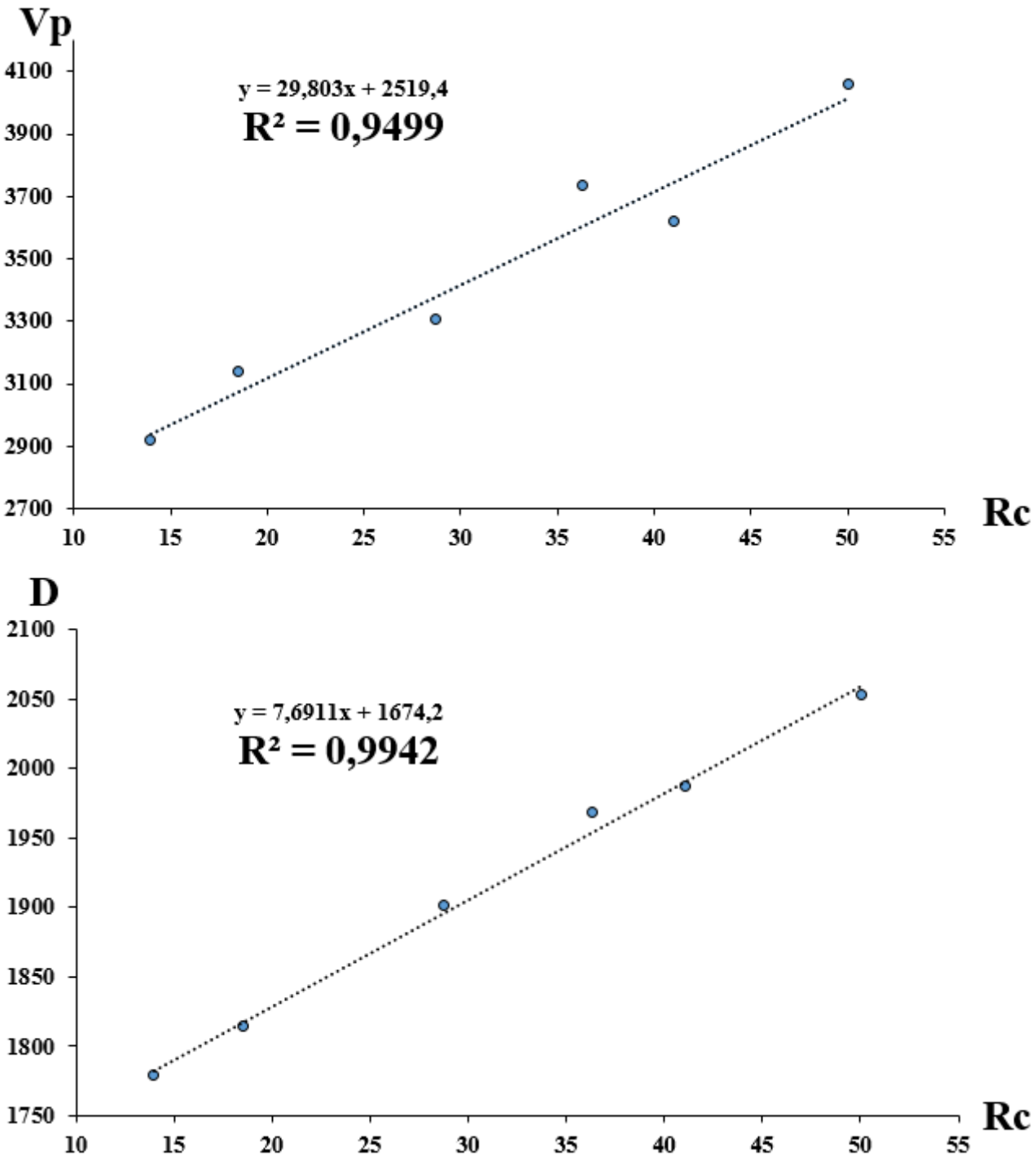

Figure 9

Correlation curves between compressive strength (Rc) with P-wave velocity (Vp) and compressive strength with bulk density (D) of synthesized geopolymers

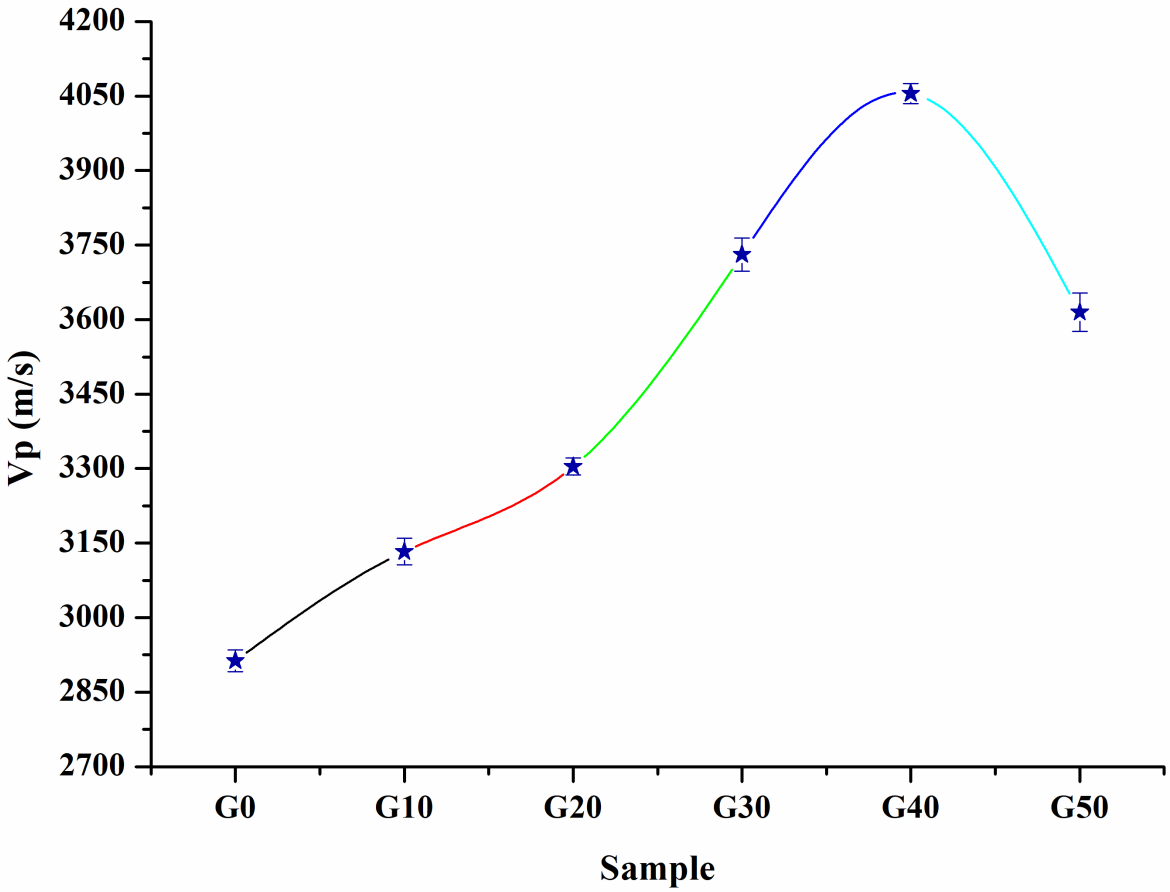

Figure 10

P-wave velocity evolution on synthesized geopolymers as a function of the perlite content

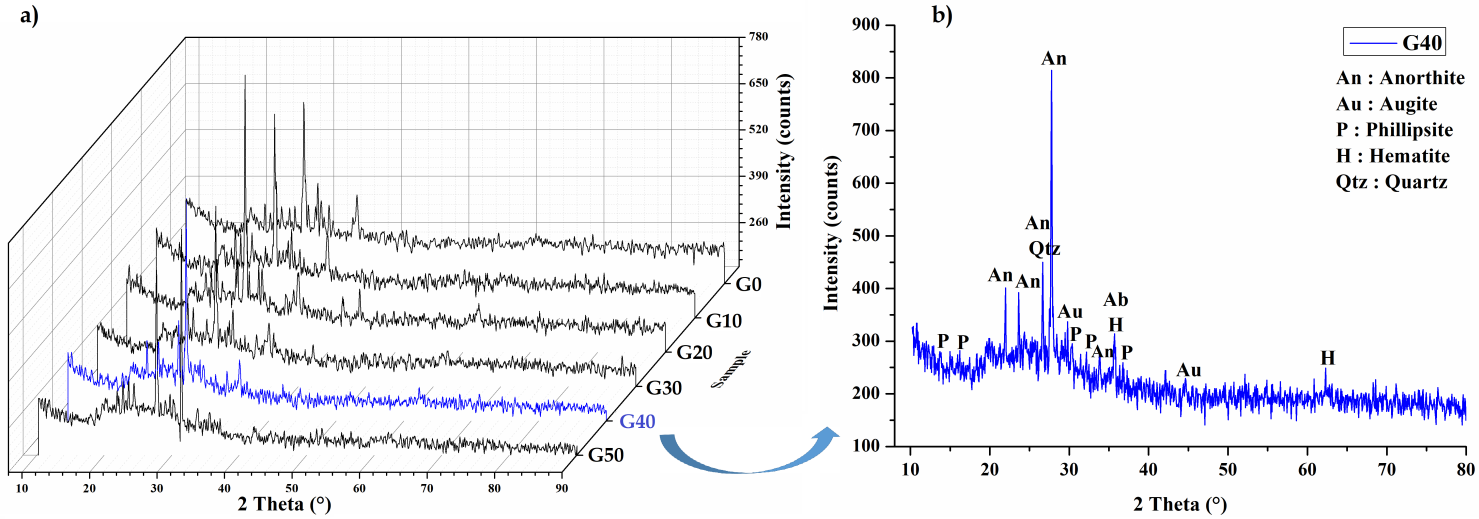

Figure 11

FT-IR spectrum of raw materials compared to that of optimal geopolymers (G40)

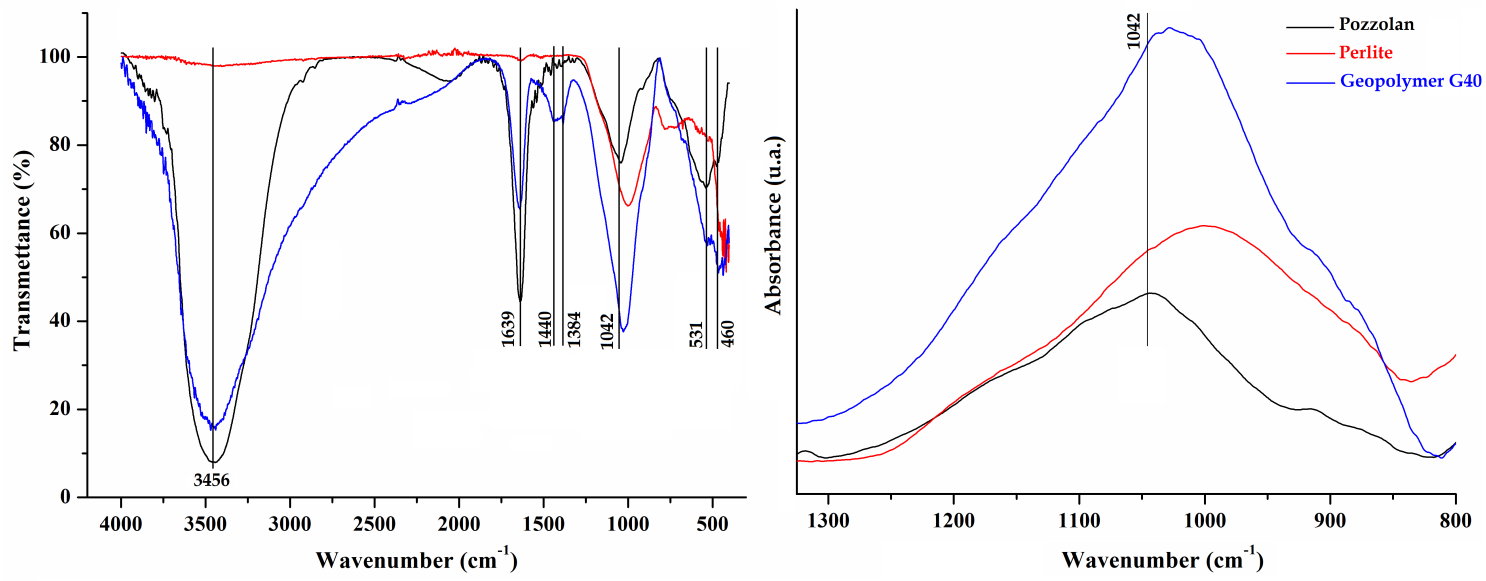

Figure 12

FT-IR spectrum of raw materials compared to that of optimal geopolymers (G40)

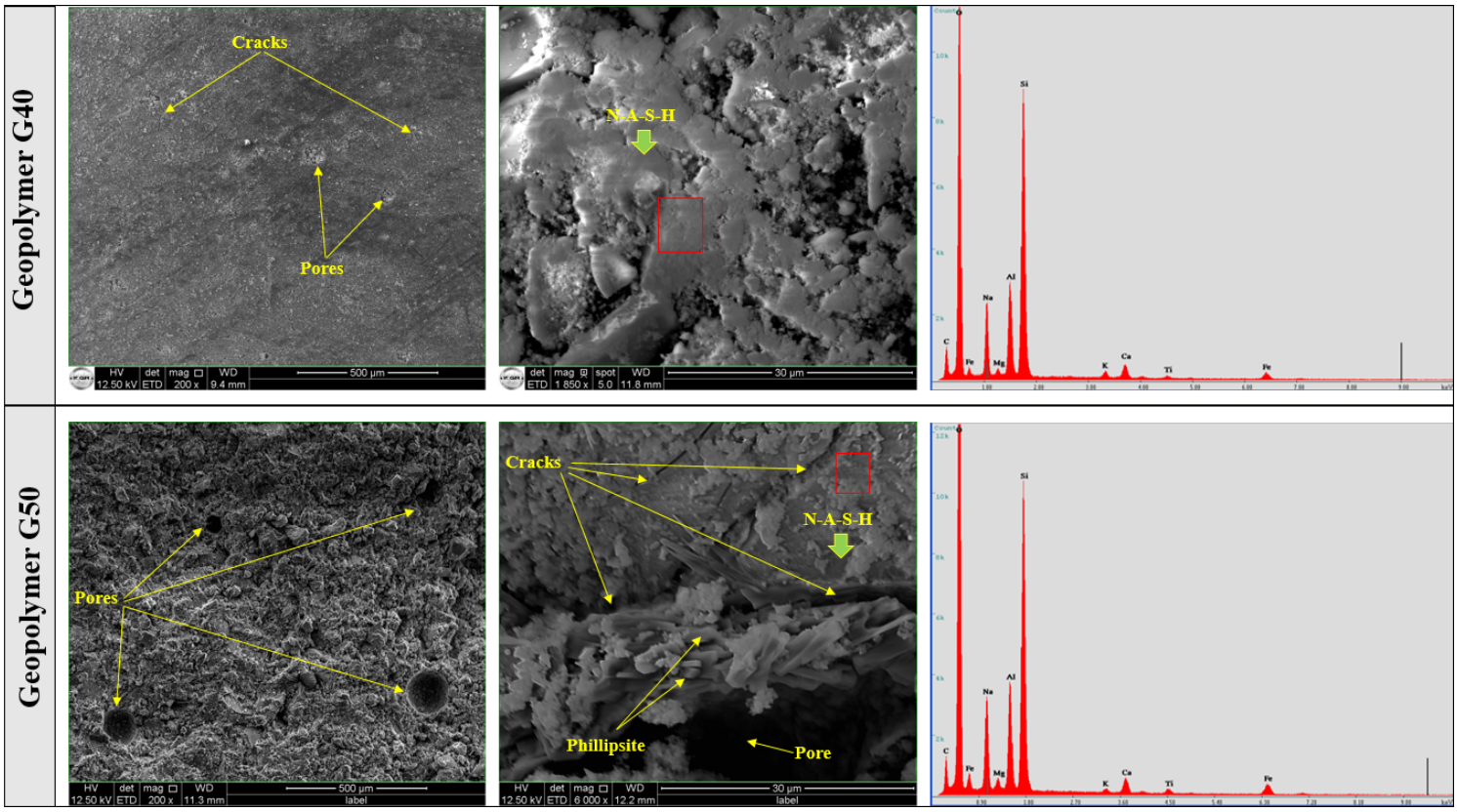

Figure 13

Typical SEM morphologies with EDS chemical analysis of G40 and G50 geopolymers at the age 28d.

Supplementary Files

This is a list of supplementary files associated with this preprint. Click to download.

- Table1.xlsx